ARMY RESEARCH LABORATORY

Permanent Magnet Solenoid: A Catalog of Field Profiles

Anu Tilak, Herbert A. Leupold and Ernest Potenziani II

ARL-TR-1123 September 1996

NOTICES

Disclaimers

REPORT DOCUMENTATION PAGE

Form Approved
OMB NO. 0704-0188

1. AGENCY USE ONLY *(Leave blank)*	2. REPORT DATE	3. REPORT TYPE AND DATES COVERED
	September 1996	Technical Report

4. TITLE AND SUBTITLE

PERMANENT MAGNET SOLENOID: A CATALOG OF FIELD PROFILES

5. FUNDING NUMBERS

6. AUTHOR(S)

Anu Tilak, Herbert A. Leupold and Ernest Potenziani II

7. PERFORMING ORGANIZATION NAMES(S) AND ADDRESS(ES)

US Army Research Laboratory (ARL)
Physical Sciences Directorate (PSD)
ATTN: AMSRL-PS-PC
Fort Monmouth, NJ 07703-5601

8. PERFORMING ORGANIZATION REPORT NUMBER

ARL-TR-1123

9. SPONSORING / MONITORING AGENCY NAME(S) AND ADDRESS(ES)

10. SPONSORING / MONITORING AGENCY REPORT NUMBER

11. SUPPLEMENTARY NOTES

12a. DISTRIBUTION / AVAILABILITY STATEMENT

Approved for public release; distribution is unlimited.

12 b. DISTRIBUTION CODE

13. ABSTRACT *(Maximum 200 words)*

Permanent magnet solenoids that employ radially oriented cladding to confine flux have found several applications of late. As the design of these solenoids becomes routine, it is inevitable that one must be able to quickly assess the feasibility of using the same in more complex gadgetry. Accordingly, this report compiles a catalog of permanent magnet solenoids and presents the required field in terms of aspect ratio, bulk and weight. An introduction to sculpting the field profile, if the design so demands, is also presented.

14. SUBJECT TERMS

Magnets; permanent magnets; permanent magnet solenoids

15. NUMBER IF PAGES

18

16. PRICE CODE

17. SECURITY CLASSIFICATION OF REPORT	18. SECURITY CLASSIFICATION OF THIS PAGE	19. SECURITY CLASSIFICATION OF ABSTRACT	20. LIMITATION OF ABSTRACT
Unclassified	Unclassified	Unclassified	UL

NSN 7540-01-280-5500

Standard Form 298 (Rev. 2-89)
Prescribed by ANSI Std. 239-18
298-102

TABLE OF CONTENTS

LIST OF FIGURES

INTRODUCTION

In millimeter wave devices, a solenoidal magnetic field is usually employed to ensure charged particle beam focussing.[1-4] The magnetic field is often provided by electrical solenoids that tend to be heavy and bulky and require cumbersome power supplies. The reduction of size and weight of millimeter wave devices has been increasingly emphasized, especially for military applications. Permanent magnet solenoids that employ radially oriented cladding magnets to confine flux produced by axially oriented supply magnets have been the subject of recent studies.[5-8] In addition, such clad magnetic structures have found applications in many other devices; for example, magnetic resonance imagers,[9] an electron filter magnet[10] and an X-ray/UV image sensor.[11]

The nature of the application dictates the strength of the desired field and the dimensions of the work space. These, in turn, determine the dimensions of the solenoid and the configurations of its components. Recent applications have required the ability to design many solenoids of varying specifications, through the use of a standard set of basic components.

Accordingly, it was decided to compile a catalog of permanent magnet solenoids to be used as a handy reference by the user in need of such a device. It provides basic information with regards to mass, volume and workspace fields and affords the user a basis for assessing, a priori, the pros and cons of the permanent magnet design over its electrical counterpart.

THEORY

Figure 1 shows a clad cylindrical permanent magnet structure, where the flux is provided by an axially magnetized permanent magnet shell, $\boldsymbol{a}$, encompassing the working space, $\boldsymbol{w}$. The shell is

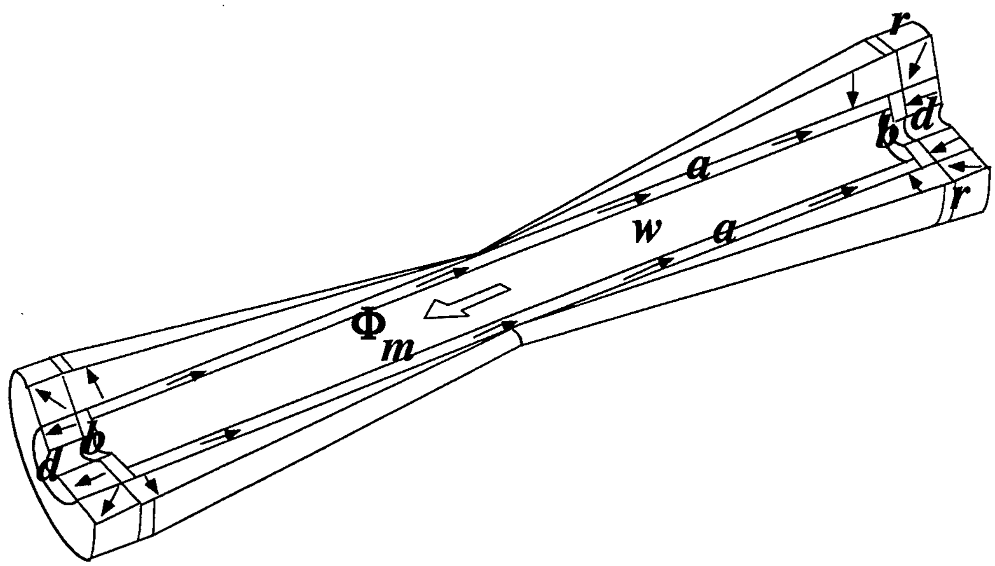

Figure 1: Permanent Magnet Solenoid

capped at its ends by iron discs, $\boldsymbol{b}$, which guide all of the magnet's flux Φ_m into $\boldsymbol{w}$. Figure 2 summarizes the calculation of the supply magnet thickness from the desired field and the dimensions of the working space. From Ampere's Law and the assumption of perfect flux confinement, we have

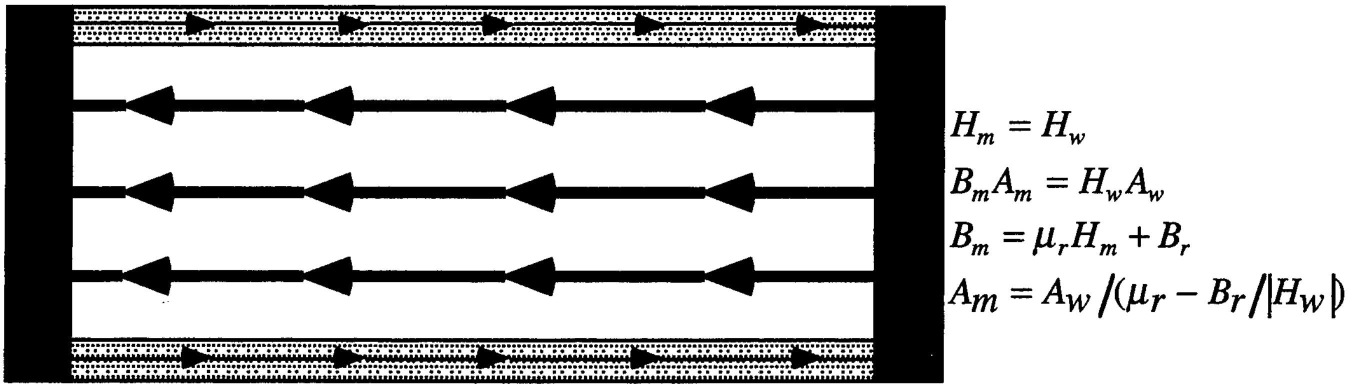

Figure 2: Configuration of Supply Magnet and Pole Pieces in the Workspace

$$\Phi_m = \Phi_W$$

$$H_m = H_W \tag{1}$$

where Φ_W is the flux in the working space, H_m is the field within the supply magnet and H_W is the field in the working space. Equating the flux inside the supply magnet to the flux within the working space, we have

$$B_m A_m = H_W A_W \tag{2}$$

where

$$B_m = \mu_r H_m + B_r \tag{3}$$

and A_m and A_W are the cross-sectional areas of the supply magnet and of the working space, respectively. μ_r denotes the slope of the demagnetization curve of the magnet material used and is approximately 1 for rigid permanent magnets. Substituting for B_m in Eq. (2) and solving for A_m we obtain

$$A_m = A_W / (\mu_r - B_r / |H_W|) \tag{4}$$

Equation (4) is written in the form shown to obviate the need to include the sign of H_m, since $H_m < 0$. The outer radius of the supply magnet is determined by A_m through the expression

$$A_m = \pi\left(r_o^2 - r_i^2\right) \tag{5}$$

where r_o and r_i are the outer and inner radii of the supply magnet, respectively.

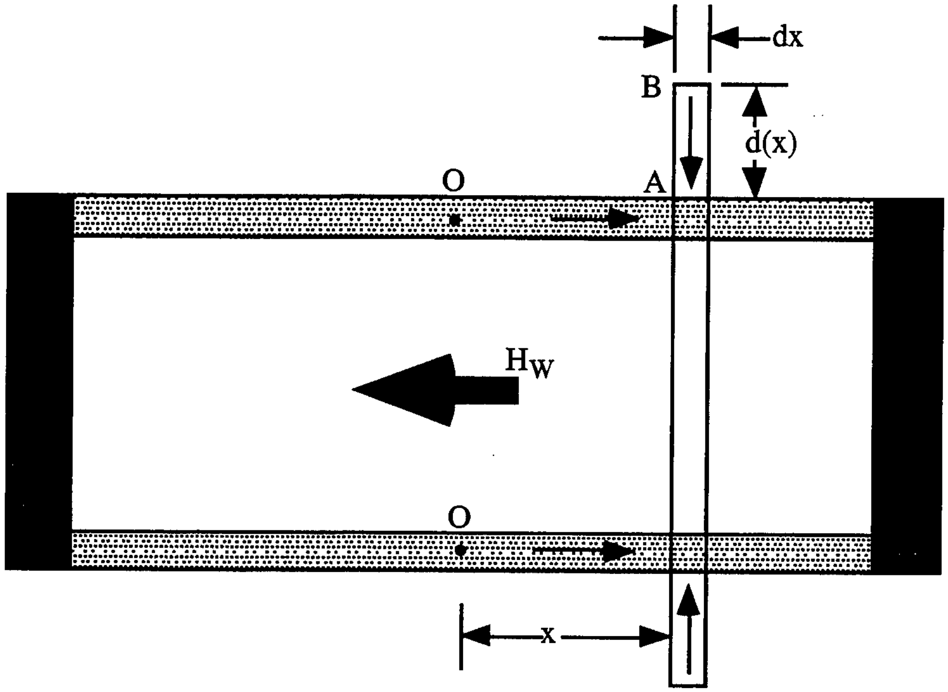

$H_c d = H_m x$

$d = H_w x / H_c$

Figure 3: Cladding Magnet Construction

To keep the flux confined to A_W we need a tapered, radially oriented cladding magnet encasing the annular longitudinal supply magnet. The supply magnet flux must be confined by a cladding magnet of unknown thickness d(x), shown in Fig. 3. The thickness of the cladding magnet is determined by the circuital form of Ampere's Law, which states that, in the absence of linking currents, $\oint H \cdot dl = 0$ around a closed loop, where dl is an infinitesimal length in the direction of the closed path and H is the magnetic field along the same path. Therefore,

$$0 = \oint H \cdot dl = H_W x + H_C d + H_{ext}(BO) \tag{6}$$

where H_C is the radial field in the cladding magnet and H_{ext} is the field outside, which is zero by hypothesis. Hence,

$$d = -H_m x / H_C \tag{7}$$

where H_C is just the magnet coercivity and d is the cladding thickness at any point x. Equation (7) yields the cladding thickness at any point along the device for $0 \le x \le L$ where L is the total length of the structure.

Next, to prevent end losses we must have pole pieces. We find the thickness of the pole pieces by equating the flux in the working space to the flux, Φ_p, traversing the circular band that forms the circumference of the pole piece. The result is :

$$\Phi_p = H_W A_W = 2\pi r_W t_p B_p$$

$$t_p = H_w A_w / 2\pi r_w B_p \tag{8}$$

where r_w is the radius of the working space and t_p is the thickness of the pole piece. If the pole piece is to be unsaturated, B_p must be no larger than B_s, the saturation induction of the pole piece material. In our case, B_s is the saturation induction of iron (20 kG). To build in a safety factor to prevent local saturation, we multiply the resulting minimal thickness by 2 and obtain

$$t_p = H_w A_w / \pi r_w B_s \tag{9}$$

With the determination of these dimensions, the design of the solenoid can be completed.

To get maximum confinement, we must also include in the design disc-shaped bucking magnets and ring-shaped corner magnets. The thickness of the end cladding is the same as the maximum cladding thickness, $t_c(\max)$, calculated for $x = L$ in Eq. (7)

FINITE ELEMENT ANALYSIS

To cover a wide range of requirements, solenoids were modeled for working space fields ranging from 500G to 6500G, and aspect ratios ranging from 0.5 to 10.0. Here, aspect ratio is defined as the ratio of length to diameter of the working space. All the solenoids modeled had a working space diameter of 2.0 cm and were made of Nd-Fe-B. A remanence of 12 kG for all permanent magnet materials and density of 8.3 g/cc for all materials was assumed in the entire design.

Finite element analysis was performed using 2D magnetic analysis software, version 13.1, from the MacNeal Schwendler Corporation. A typical plot of the magnetic flux is shown in Fig. 4.

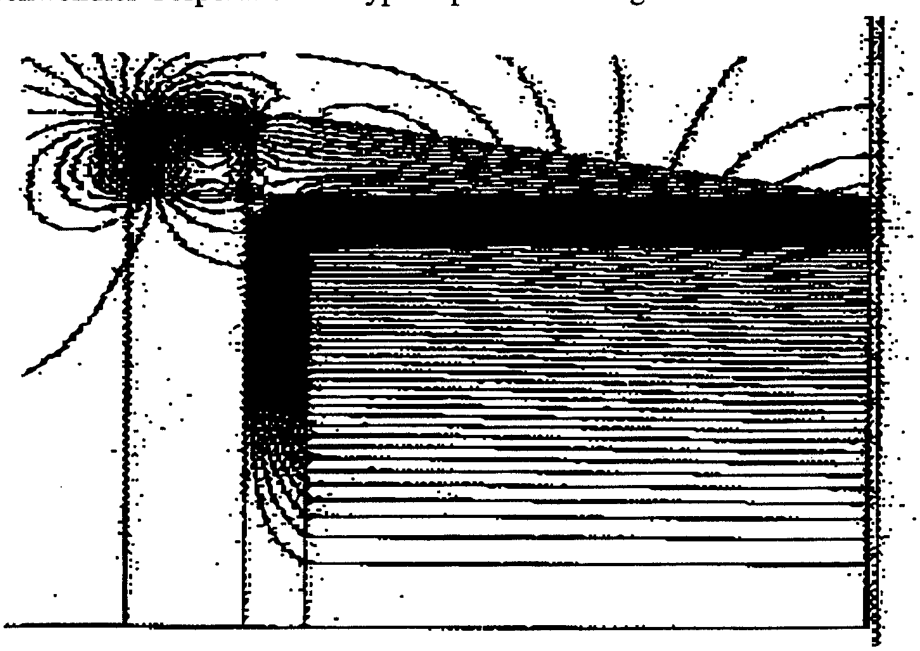

Figure 4: Magnetic Flux Distribution in a Permanent Magnet Solenoid

RESULTS

The flux plot of Fig. 4 shows excellent flux confinement by the radially oriented cladding magnets and the disc-shaped bucking magnets. There is some leakage of flux at the corners near the ring-shaped bucking magnets. This issue has been dealt with elsewhere[12] and can be reduced with a modification to the basic solenoid if the leakage presents a problem to instrumentation placed in that region.

Figures 5-11 show the field profiles along the axis of the solenoids, sequentially, for fields ranging from 500 gauss to 6500 gauss in increments of 1000 gauss. The field estimated by the finite element calculation is indeed, on the average, the field expected from the design. It would seem from a quick glance at the field profiles, however, that there is a significant deviation from the desired field along the axis. The fields are somewhat higher near the center of the solenoid and drop off considerably towards the ends of the axis. For small aspect ratios, i.e. ≤ 1, the percentage of error ranges anywhere from 1.5% for small fields to 3.0% for the larger fields. For larger aspect ratios these percentages of error are less impressive, starting from a mere 5.2% for a 500G solenoid and rising to to 38.5% for our longest design, an aspect ratio of 10, for the highest field in this study, 6500 G. If such deviations in polar axis fields are deemed too large, remedies are available to make the field profile more uniform.[12]

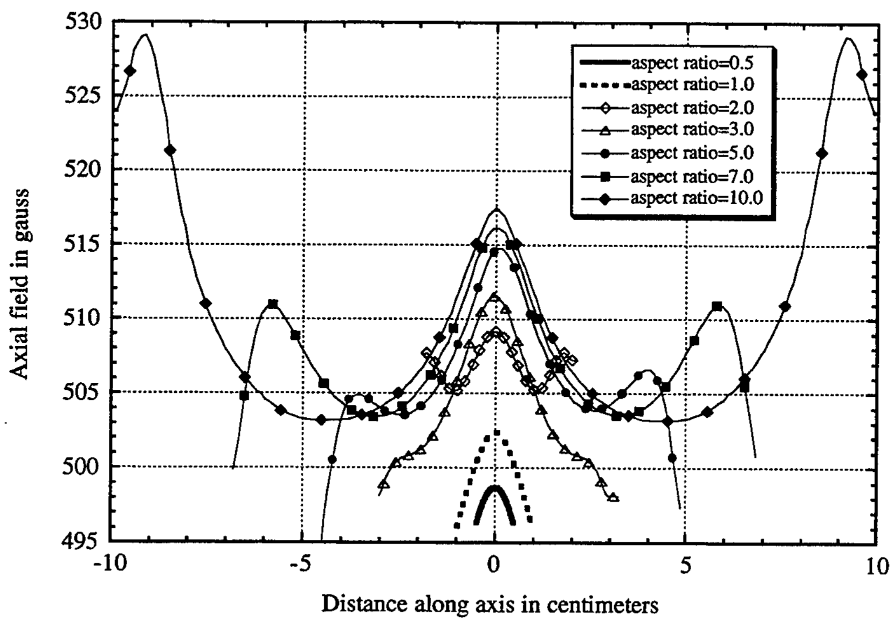

Figure 5: Axial Fields for a 500 gauss Solenoid

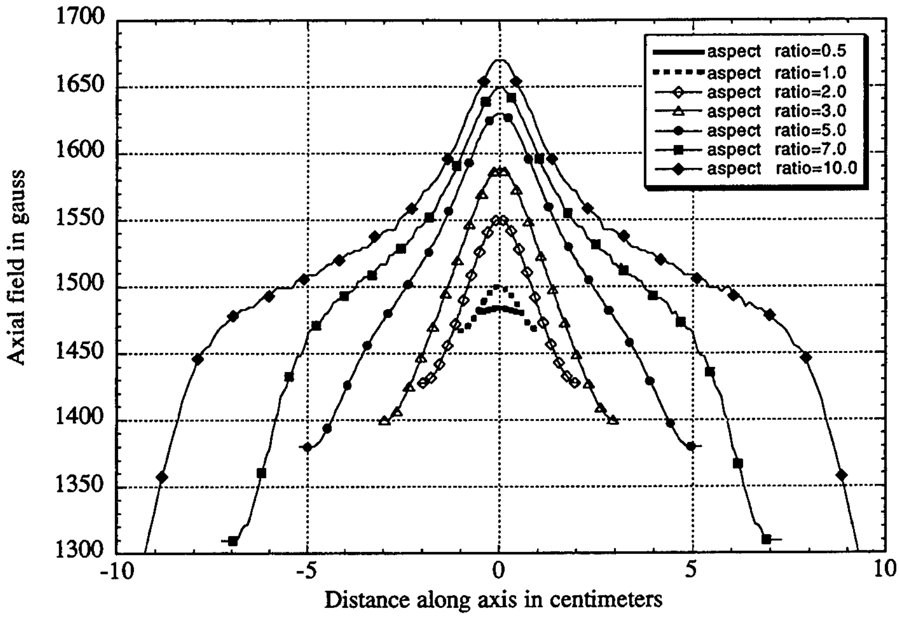

Figure 6: Axial Fields for a 1500 gauss Solenoid

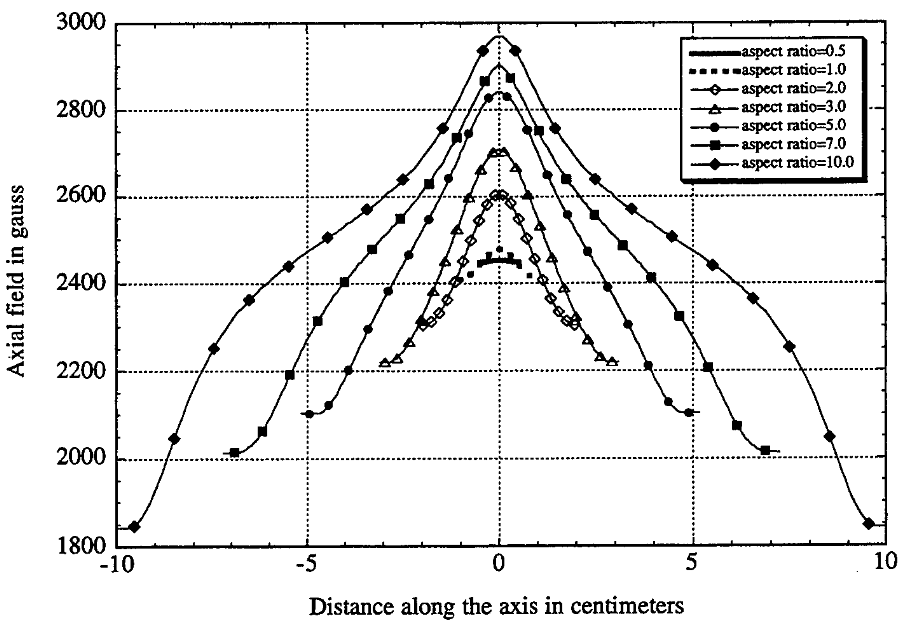

Figure 7: Axial Fields for a 2500 gauss Solenoid

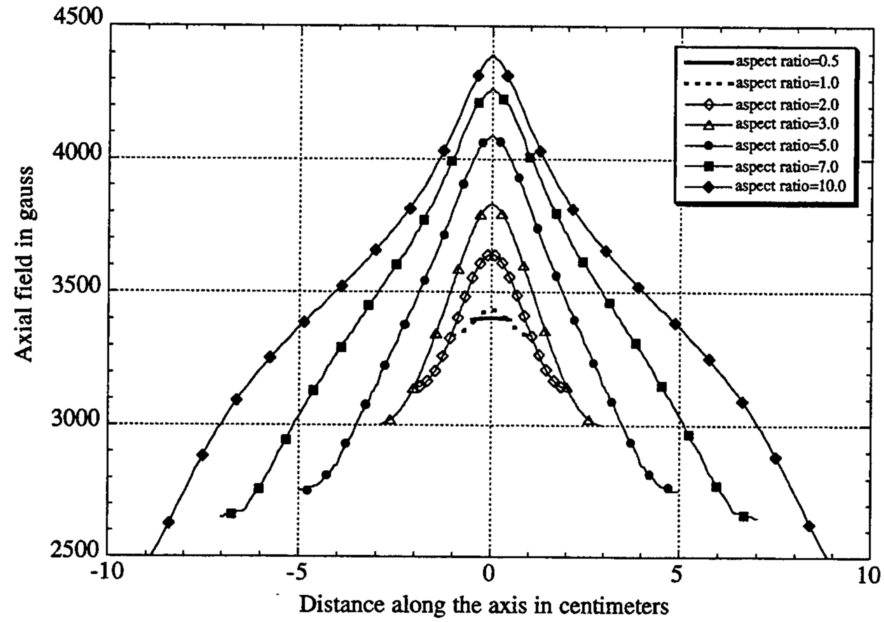

Figure 8: Axial Fields for a 3500 gauss Solenoid

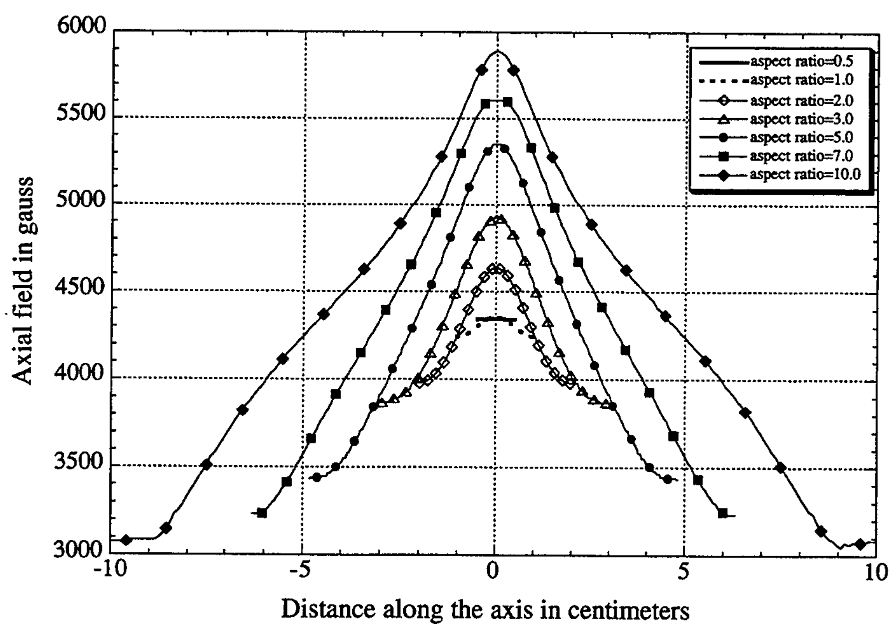

Figure 9: Axial Fields for a 4500 gauss Solenoid

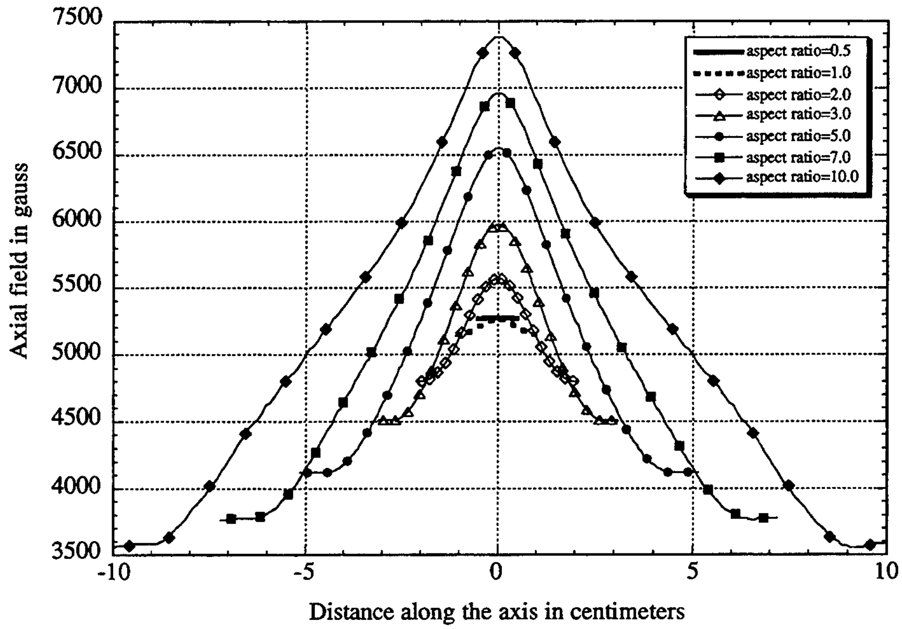

Figure 10: Axial Fields for a 5500 gauss Solenoid

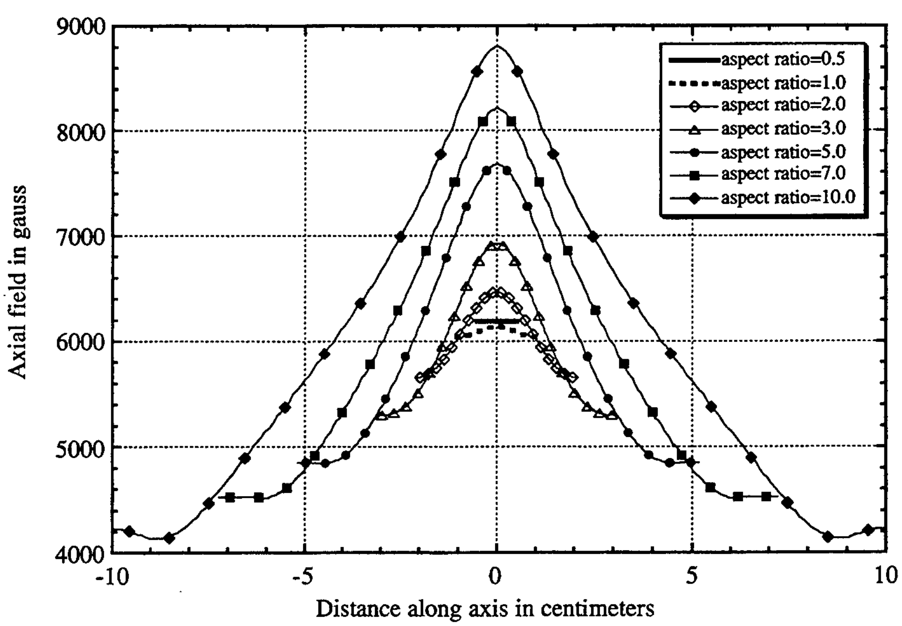

Figure 11: Axial Fields for a 6500 gauss Solenoid

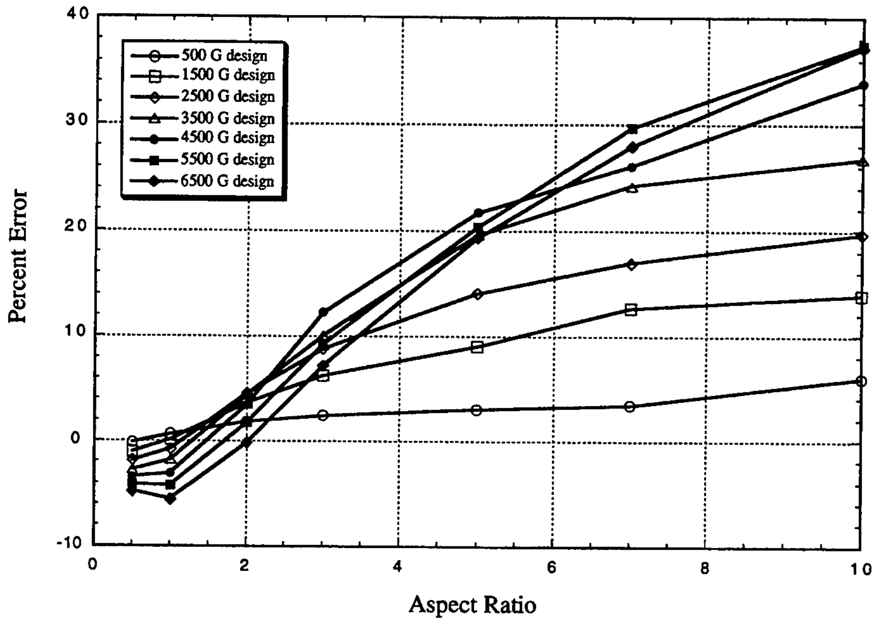

Figure 12: Percentage of Error in the Obtained Field as a Function of Aspect Ratio

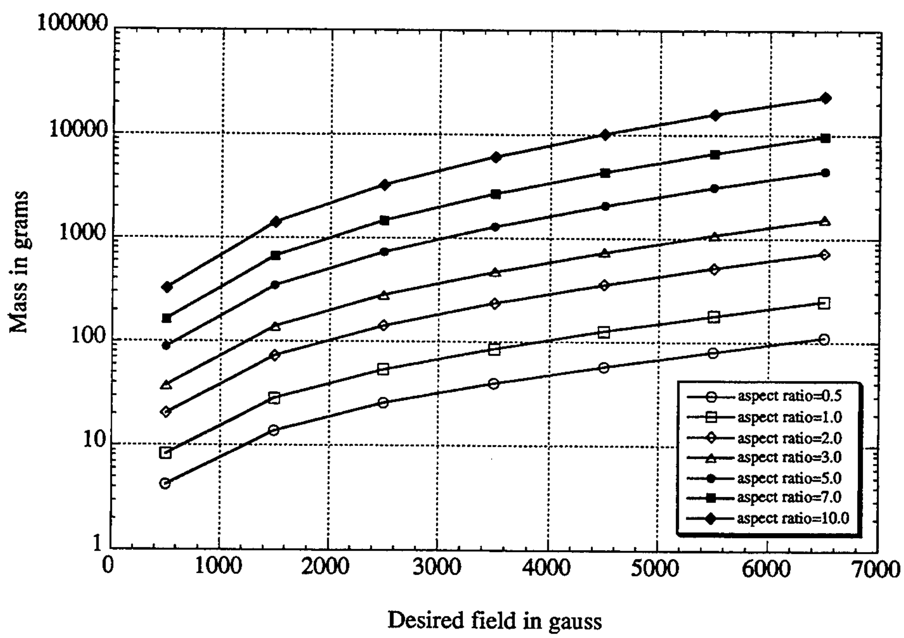

Figure 13: Solenoid Mass as a Function of Desired Field

Figure 12 summarizes the difference in the required fields and the peak fields at the center of the solenoid, expressed as a percentage of error, as a function of aspect ratio. If the length of the working space is small in comparison with the inner radius of the solenoid, annular confinement of flux is favored.

CONCLUSION

A permanent magnet solenoid can be designed accurately for any desired field. If field uniformity is the criterion for evaluating the success of the design, the permanent magnet solenoid is best for small fields and aspect ratios. As the requirements shift towards higher working space fields, one must sacrifice uniformity in field profile, particularly if the demand is for a working space that is several fold longer than it is wide. Figure 13 is the designer's guide to the increase in the mass of the solenoid as one demands a larger field.

It would appear from studying the magnetic field profiles in Figs. 5-11 as well as the summary presented in Fig. 12, that field uniformity in the interior of the solenoid can be rather poor, particularly for high aspect ratios. This arises due to imperfect cladding at the ends. Many applications find this field gradient acceptable while others are stringent in their demands for a uniform field. For the latter, the permanent magnet solenoid is still a viable alternative. A simple modification, discussed in detail elsewhere,[9,12] can improve the field profile dramatically. This is

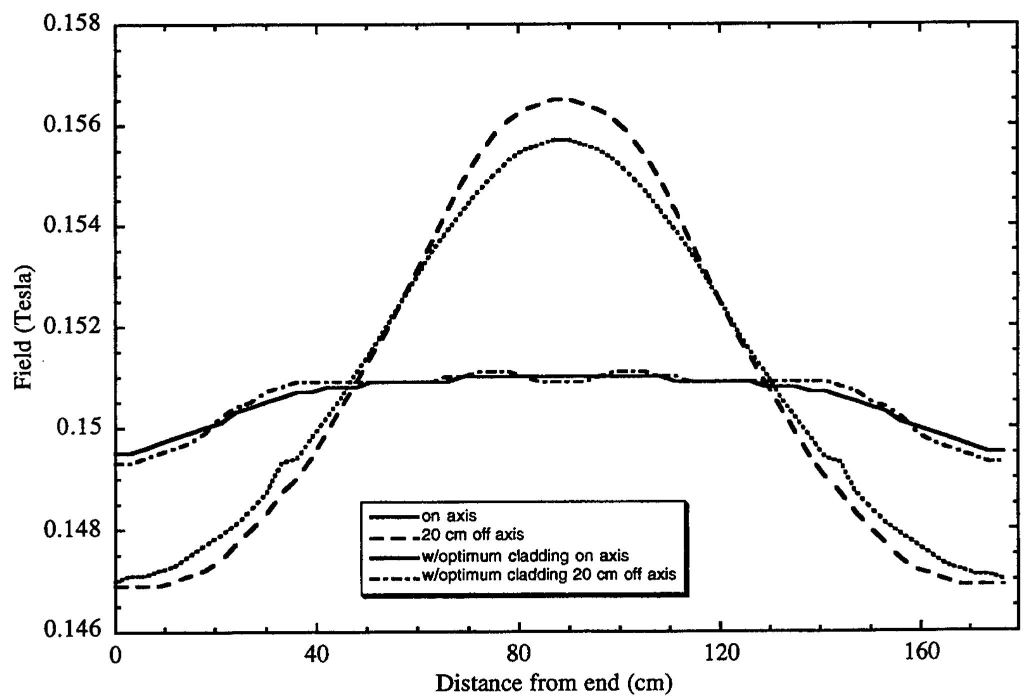

Figure 14: Axial magnetic field profile in a cladding compensated solenoid

accomplished by altering the thickness of the cladding magnet. It can be done geometrically. The correction consists of increasing the cladding thickness Δt according to the formula:

$$\Delta t = (H_d - H_a)t / H_a \tag{10}$$

where H_d is the desired field and H_a is the actual field. Figure 14 shows the axial field as a function of distance from one end in a sample solenoid. The much improved field uniformity obtained after a simple correction to the cladding slope is made is also included. The deviation from the average field in the unaltered solenoid is 3.0% and is reduced to less than 0.01% upon geometric modification of the cladding.

It is also possible to vary the cladding parametrically.[3] B_r, the remanence of the cladding magnets, can be gradually increased in the manner shown below:

$$\Delta B_r = H_a \Delta t / t \tag{11}$$

where Δt is the increment in cladding thickness t determined by Eq. (10).

REFERENCES

1. R. M W Strnat, J. P. Clarke, H. A. Leupold, and A. Tauber, J. Appl. Phys. 61, 3463 (1982).
2. A. B. C. Morcos, E. Potenziani II, and H. A. Leupold, IEEE Trans. Magn., vol. MAG-22, no. 5, p. 1066, 1986.
3. J. P. Clarke and H. A. Leupold, IEEE Trans. Magn., vol. MAG-22, no. 5, p. 1063, 1986.
4. J. P. Clarke, E. Potenziani II, and H. A. Leupold. J. Appl. Phys 61, 3468 (1987).
5. A. Tilak, D. J. Basarab, H. A. Leupold, and E. Potenziani II, Magnetic Field Source for Bi-chambered Electron Beam Devices, Technical Report, SLCET-TR-91-11, U. S. Army Research Laboratory, Fort Monmouth, New Jersey (1992).
6. H. A. Leupold, E. Potenziani II, D. P. Meyers, and D. S. Furuno, A Novel Permanent Magnet Electron Beam Guide, Technical Report, ARL-TR-427, Army Research Laboratory, Fort Monmouth, New Jersey (1995).
7. D. S. Furuno, D.P. Myers, K. T. Lancaster, H.A. Leupold, E. Potenziani II, A. Nanji, and G. K. Sadakane, IEDM Technical Dig., 211 (1995).
8. H. A. Leupold, A Lightweight Electron Beam Focussing Structure for CORPSAM Missile Radars, Proceedings: Army Science Conference, June 1996, to be published.
9. E. Potenziani II and H. A. Leupold, IEEE. Trans. Magn., vol. MAG-22, no. 5, p. 1078, 1986.
10. Coey, W.D.M., Elements of Permanent Magnet Design, Chapter in Rare Earth Permanent Magnets, Oxford University Press, May 1996.
11. H. A. Leupold, E. Potenziani II, and J. L. Lowrance, IEEE Trans. Magn., vol. 28, no. 5, p. 3048, (1992).
12. H. A. Leupold, and E. Potenziani II, A Permanent Magnet Circuit Design Primer, Technical Report, ARL-TR-946, U. S. Army Research Laboratory, Fort Monmouth, New Jersey (1996).

ARMY RESEARCH LABORATORY
PHYSICAL SCIENCES DIRECTORATE
MANDATORY DISTRIBUTION LIST

Defense Technical Information Center*
ATTN: DTIC-OCC
8725 John J. Kingman Rd STE 0944
Fort Belvoir, VA 22060-6218
(*Note: Two DTIC copies will be sent
from STINFO office, Ft. Monmouth, NJ)

Director
US Army Material Systems Analysis Actv
ATTN: DRXSY-MP
(1) Aberdeen Proving Ground, MD 21005

Commander, AMC
ATTN: AMCDE-SC
5001 Eisenhower Ave.
(1) Alexandria, VA 22333-0001

Director
Army Research Laboratory
ATTN: AMSRL-D (John W. Lyons)
2800 Powder Mill Road
(1) Adelphi, MD 20783-1197

Director
Army Research Laboratory
ATTN: AMSRL-DD (COL Thomas A. Dunn)
2800 Powder Mill Road
(1) Adelphi, MD 20783-1197

Director
Army Research Laboratory
2800 Powder Mill Road
Adelphi, MD 20783-1197
(1) AMSRL-OP-SD-TA (ARL Records Mgt)
(1) AMSRL-OP-SD-TL (ARL Tech Library)
(1) AMSRL-OP-SD-TP (ARL Tech Publ Br)

Directorate Executive
Army Research Laboratory
Physical Sciences Directorate
Fort Monmouth, NJ 07703-5601
(1) AMSRL-PS-A (V. Rosati)
(1) AMSRL-PS-T (M. Hayes)
(22) Originating Office

Advisory Group on Electron Devices
ATTN: Documents
Crystal Square 4
1745 Jefferson Davis Highway, Suite 500
(2) Arlington, VA 22202

Commander, CECOM
R&D Technical Library
Fort Monmouth, NJ 07703-5703
(1) AMSEL-IM-BM-I-L-R (Tech Library)
(3) AMSEL-IM-BM-I-L-R (STINFO Ofc)

Deputy for Science & Technology
Office, Asst Sec Army (R&D)
(1) Washington, DC 20310

HQDA (DAMA-ARZ-D/
Dr. F.D. Verderame)
(1) Washington, DC 20310

Director
Naval Research Laboratory
ATTN: Code 2627
(1) Washington, DC 20375-5000

USAF Rome Laboratory
Technical Library, FL2810
ATTN: Documents Library
Corridor W, STE 262, RL/SUL
26 Electronics Parkway, Bldg. 106
Griffiss Air Force Base
(1) NY 13441-4514

Dir, ARL Battlefield
Environment Directorate
ATTN: AMSRL-BE
White Sands Missile Range
(1) NM 88002-5501

Dir, ARL Sensors, Signatures,
Signal & Information Processing
Directorate (S3I)
ATTN: AMSRL-SS
2800 Powder Mill Road
(1) Adelphi, MD 20783-1197

Dir, CECOM Night Vision/
Electronic Sensors Directorate
ATTN: AMSEL-RD-NV-D
(1) Fort Belvoir, VA 22060-5806

Dir, CECOM Intelligence and
Electronic Warfare Directorate
ATTN: AMSEL-RD-IEW-D
Vint Hill Farms Station
(1) Warrenton, VA 22186-5100

Cdr, Marine Corps Liaison Office
ATTN: AMSEL-LN-MC
(1) Fort Monmouth, NJ 07703-5033